Nephrogenic diabetes insipidus in mice lacking aquaporin-3 water channels

Tonghui Ma, Yuanlin Song, Baoxue Yang, Annemarie Gillespie, Elaine J. Carlson, Charles J. Epstein, and A. S. Verkman*

Departments of Medicine, Physiology, and Pediatrics, Cardiovascular Research Institute, University of California, San Francisco, CA 94143-0521

Edited by Maurice B. Burg, National Institutes of Health, Bethesda, MD, and approved February 15, 2000 (received for review November 16, 1999)

Aquaporin-3 (AQP3) is a water channel expressed at the basolateral plasma membrane of kidney collecting-duct epithelial cells. The mouse AQP3 cDNA was isolated and encodes a 292-amino acid water/glycerol-transporting glycoprotein expressed in kidney, large airways, eye, urinary bladder, skin, and gastrointestinal tract. The mouse AQP3 gene was analyzed, and AQP3 null mice were generated by targeted gene disruption. The growth and phenotype of AQP3 null mice were grossly normal except for polyuria. AQP3 deletion had little effect on AQP1 or AQP4 protein expression but decreased AQP2 protein expression particularly in renal cortex. Fluid consumption in AQP3 null mice was more than 10-fold greater than that in wild-type litter mates, and urine osmolality (<275 milliosmol) was much lower than in wild-type mice (>1,200 milliosmol). After 1-desamino-8-D-arginine-vasopressin administration or water deprivation, the AQP3 null mice were able to concentrate their urine partially to ≈30% of that in wild-type mice. Osmotic water permeability of cortical collecting-duct basolateral membrane, measured by a spatial filtering optics method, was >3-fold reduced by AQP3 deletion. To test the hypothesis that the residual concentrating ability of AQP3 null mice was due to the inner medullary collecting-duct water channel AQP4, AQP3/AQP4 double-knockout mice were generated. The double-knockout mice had greater impairment of urinary-concentrating ability than did the AQP3 single-knockout mice. Our findings establish a form of nephrogenic diabetes insipidus produced by impaired water permeability in collecting-duct basolateral membrane. Basolateral membrane aquaporins may thus provide blood-accessible targets for drug discovery of aquaretic inhibitors.

water transport | AQP3 | kidney | urinary-concentrating mechanism | polyuria

Aquaporin-3 (AQP3, originally called glycerol intrinsic protein, GLIP, based on its glycerol-transport function) was cloned from rat kidney by our laboratory (1) as well as by Ishibashi *et al.* (2) and Echevarria *et al.* (3). AQP3 is a relatively weak transporter of water but functions as an efficient glycerol transporter (4). Reflection coefficient measurements (5) and mutagenesis studies (6) suggested that water and glycerol share a common pathway through the AQP3 protein, although inhibition experiments were interpreted as suggesting different pathways (7). Immunocytochemistry in rat showed AQP3 protein expression in basolateral membrane of kidney collecting duct and large airways, as well as in several tissues that are thought not to have an important water-transporting role including urinary bladder, conjunctiva, and epidermis (8–11). Recent studies report strong AQP3 expression in various regions of the gastrointestinal tract including small intestine (12). Another unique feature of AQP3 is its gene structure, which is different from the water-selective mammalian aquaporins (13). AQP3, AQP7, and AQP9 have been called "aquaglyceroporins" because of their relatively broad solute specificity and sequence homology. The physiological role of glycerol and solute transport by the aquaglyceroporins is unknown.

AQP3 transcript and protein are expressed most strongly in kidney. In rat, AQP3 protein is constitutively expressed on basolateral membranes of principal cells in cortical and outer medullary collecting duct (8, 9, 14, 15). AQP4 protein is also expressed at the basolateral membrane of collecting-duct epithelial cells but mostly in inner medullary collecting-duct segments (9, 16). Principal and inner medullary collecting-duct cells also express AQP2, a water channel that undergoes vasopressin-regulated trafficking between an intracellular vesicular compartment and the cell apical plasma membrane. We previously showed that transgenic mice lacking AQP4 were not polyuric but manifested a very mild defect in maximum urinary-concentrating ability in response to water deprivation (17). Transepithelial osmotic water permeability in the microperfused, vasopressin-stimulated inner medullary collecting duct of AQP4 null mice was 4-fold lower than in wild-type mice (18), indicating that AQP4 is the dominant basolateral membrane water channel in inner medullary collecting duct. Because the majority of fluid in the antidiuretic kidney is extracted from the lumen in cortical collecting duct, it was hypothesized that AQP3 might be more critical than AQP4 for the formation of concentrated urine. The kidney also contains AQP1 in proximal tubule, thin descending limb of Henle, and outer medullary vasa recta. AQP1 null mice manifest severely impaired urinary-concentrating ability (19) associated with reduced proximal tubule fluid absorption (20) and defective countercurrent exchange caused by low water permeability in thin descending limb of Henle (21) and vasa recta (22).

The purpose of this study was to determine the role of AQP3 in the urinary-concentrating mechanism by generation and analysis of AQP3 null mice. AQP3 is the first aquaglyceroporin to be deleted in mice. The AQP3 null mice had normal perinatal survival and postnatal growth but were remarkably polyuric and polydipsic. The mechanisms responsible for the polyuria in AQP3 null mice were evaluated by *in vivo* 1-desamino-8-D-arginine-vasopressin (DDAVP) and water-deprivation challenges, measurement of osmotic water permeability in basolateral membrane of cortical collecting duct, immunoblot analysis of renal aquaporin expression, and generation and analysis of AQP3/AQP4 double-knockout mice. The unique form of nephrogenic diabetes insipidus in the AQP3 null mice indicates that AQP3-mediated water transport across the basolateral membrane of collecting-duct epithelium is important for the formation of concentrated urine.

Methods

cDNA Cloning and Genomic Analysis of Mouse AQP3. The mouse AQP3 cDNA sequence was obtained by searching the National

This paper was submitted directly (Track II) to the PNAS office.

Abbreviations: mosM, milliosmol; DDAVP, 1-desamino-8-D-arginine-vasopressin; kb, kilobase.

Data deposition: The sequences reported in this paper have been deposited in the GenBank database (accession nos. AF104416 for AQP3 cDNA and AF104417 for the AQP3 gene).

*To whom reprint requests should be addressed. E-mail: verkman@itsa.ucsf.edu.

The publication costs of this article were defrayed in part by page charge payment. This article must therefore be hereby marked "*advertisement*" in accordance with 18 U.S.C. §1734 solely to indicate this fact.

Article published online before print: *Proc. Natl. Acad. Sci. USA*, 10.1073/pnas.080499597. Article and publication date are at www.pnas.org/cgi/doi/10.1073/pnas.080499597

Center for Biotechnology Information mouse expressed sequence tag database with the rat AQP3 sequence. Seven overlapping expressed sequence tags (AI788487, C88951, AI893394, W56935, AA270817, AI463895, and AI117780) gave a 1,649-bp continuous sequence with an 876-bp ORF encoding a 292-amino acid protein. The mouse AQP3 coding sequence was PCR amplified by using C57BL6/J mouse kidney cDNA as template and primers flanking the predicted coding sequence. For functional measurements of water and glycerol permeability, the mouse AQP3 cRNA was subcloned into oocyte expression plasmid pSP64T, and *in vitro* transcribed cRNA was expressed in *Xenopus laevis* oocytes as described (23). The structure of the mouse AQP3 gene was analyzed by PCR amplification of exon–intron–exon fragments by using C57 mouse liver genomic DNA as template. The entire cDNA coding sequence and all exon–intron boundaries were sequenced.

Generation of AQP3 Null Mice. A targeting vector for homologous recombination was constructed with a 3.5-kilobase (kb) genomic AQP3 DNA fragment containing exon 1, intron 1, and partial exon 2 (left arm) and a 1.3-kb fragment containing partial exon 3, exons 4–6, and introns 3–5 (right arm). The left and right arm genomic fragments (surrounding a 1.8-kb PolIIneobpA cassette) were PCR amplified, and a PGK-tk cassette was inserted upstream for negative selection. The targeting vector was linearized at a unique downstream *Not*I site and electroporated into CB1-4 embryonic stem cells. Transfected embryonic stem cells were selected with G418 and FIAU for 7 days, yielding three targeted clones of 196 doubly resistant colonies on PCR screening with a neo-specific sense primer and an AQP3 gene-specific antisense primer located 50 bp downstream of the targeting region. Homologous recombination was confirmed by Southern hybridization in which 10 μg of genomic DNA was digested with *Eco*RI, electrophoresed, transferred to a Nylon+ membrane (Amersham Pharmacia), and hybridized with a 0.6-kb genomic fragment (as indicated in Fig. 2*A*). Embryonic stem cells were injected into postcoitus 2.5-day eight-cell morula stage CD1 zygotes, cultured overnight to blastocysts, and transferred to pseudopregnant B6D2 females. Offspring were genotyped by PCR followed by Southern blot analysis as described above. Heterozygous founder mice containing the disrupted AQP3 gene in the germ line were bred to produce homozygous AQP3-knockout mice.

Generation of AQP3/AQP4 Double-Knockout Mice. Because the AQP3 and AQP4 genes are localized on different chromosomes in the mouse genome, AQP3/AQP4 double-knockout mice were generated by intercross of the single knockouts. Breeding of F_2 generation double-heterozygous mice yielded 8 AQP3/AQP4-knockout mice from 65 pups.

Northern Blot and Reverse Transcription–PCR Southern Blot Analysis. A multitissue mouse Northern blot (CLONTECH) was hybridized at high stringency with a ^{32}P-labeled probe corresponding to the mouse AQP3 cDNA coding sequence. For reverse transcription–PCR Southern blot analysis, first-strand cDNAs were reverse transcribed from 0.5 μg of mRNA isolated from a series of C57 mouse tissues. After normalization for template quantity by PCR with mouse β-actin primers, equal amounts ($\approx$50 ng) of each template cDNA were used for PCR amplification with AmpliTaq Gold DNA polymerase (Perkin–Elmer) and primers amplifying the AQP3 coding region. PCR products were resolved on a 1.5% agarose gel, blotted to the Nylon+ membrane, hybridized as described above, and exposed to Hyperfilm-MP at room temperature for 5 min.

Immunofluorescence and Immunoblot Analysis. Immunofluorescence localization of AQP3 protein in fixed frozen kidney sections was done with a 1:500 dilution of rabbit polyclonal serum raised against a C-terminal peptide as described (9). Immunoblot analysis of membranes from kidney homogenates was carried out with rabbit polyclonal antibodies for AQP1, AQP2, AQP3, and AQP4 as described (24).

Urine and Serum Analysis. Urine samples from 30- to 40-day-old mice were collected in mouse metabolic cages (Harvard Apparatus) for 24 h collections or by placing mice on a wire mesh platform in a clean glass beaker until spontaneous voiding was observed. In some experiments, urine samples were obtained after deprivation of food and water for up to 36 h or at 30 min after two i.p. DDAVP injections (0.4 μg/kg) 30 min apart. Urine osmolalities (by freezing point osmometry) and urine and serum chemistries were measured by the University of California San Francisco Clinical Chemistry Laboratory.

Water-Permeability Measurements. Osmotic water permeability (P_f) across the basolateral membrane of cortical collecting duct was measured by a spatial filtering microscopy method as originally described for P_f determination in planar cell monolayers (25). Spatial filtering microscopy exploits the change in cytoplasmic refractive index (and thus optical path length) produced by changes in cell volume. Cortical collecting-duct segments were obtained by perfusing mouse kidneys for 10 min with 0.1% collagenase in Hanks' balanced salt solution and then incubating fragments of dissected cortex in the same buffer for 10–15 min. Washed tubule suspensions were placed on poly-D-lysine-coated cover glasses (high molecular weight; Sigma). After incubation at 23°C for 5 min, the cover glass containing immobilized tubule segments was mounted in a perfusion chamber on the stage of an inverted epifluorescence microscope (Nikon Diaphot) equipped with a phase condenser. The illumination source consisted of a stabilized tungsten-halogen lamp, infrared blocking filter, and >560-nm cut-on filter. Transmitted light was collected with a 20× phase objective (Nikon, numerical aperture 0.4), and intensity was measured at 1,000 Hz by a photodiode (Thor Labs, Newton, NJ) interfaced to a PC computer by a 14-bit analog-to-digital converter. An adjustable diaphragm was positioned to illuminate a spot in the focal plane just larger than the diameter of a collecting duct, which was identified by its characteristic diameter and large epithelial cells. Trypan blue was used to identify viable tubules. The cover glass was perfused continuously (12–15 ml/min), and the perfusate was switched with a solenoid valve ($\approx$300-ms exchange time) between PBS and hypotonic PBS (1:1 PBS:distilled water) to induce osmotic volume changes.

Results

The AQP3 cDNA from C57BL6/J mouse kidney encodes a 31.6-kDa, 292-amino acid protein with six putative hydrophobic transmembrane domains. The deduced amino acid sequence is 95% and 96% identical to human and rat AQP3, respectively (Fig. 1*A*). Northern blot analysis revealed a single AQP3 transcript of 1.9 kb expressed in kidney (Fig. 1*B*). PCR–Southern blot analysis of a series of mouse tissues indicated a wide AQP3 mRNA distribution with strongest expression in kidney, urinary bladder, eye, skin, trachea, and gastrointestinal tract (except colon), with lower expression in testis, lung, and spleen (Fig. 1*C*). Functional analysis in *Xenopus* oocytes expressing mouse AQP3 cRNA indicated water- and glycerol-transport activity (Fig. 1*D*), in agreement with results for rat and human AQP3 (1–3). Also, as found previously (4), AQP3-expressing oocytes were less water-permeable than AQP1-expressing oocytes.

Fig. 2*A Top* shows the organization of the mouse AQP3 gene as deduced by comparison of genomic and cDNA sequences. There are six exons of lengths 118, 127, 138, 119, 215, and 164 bp in the coding region separated by five introns. The introns are

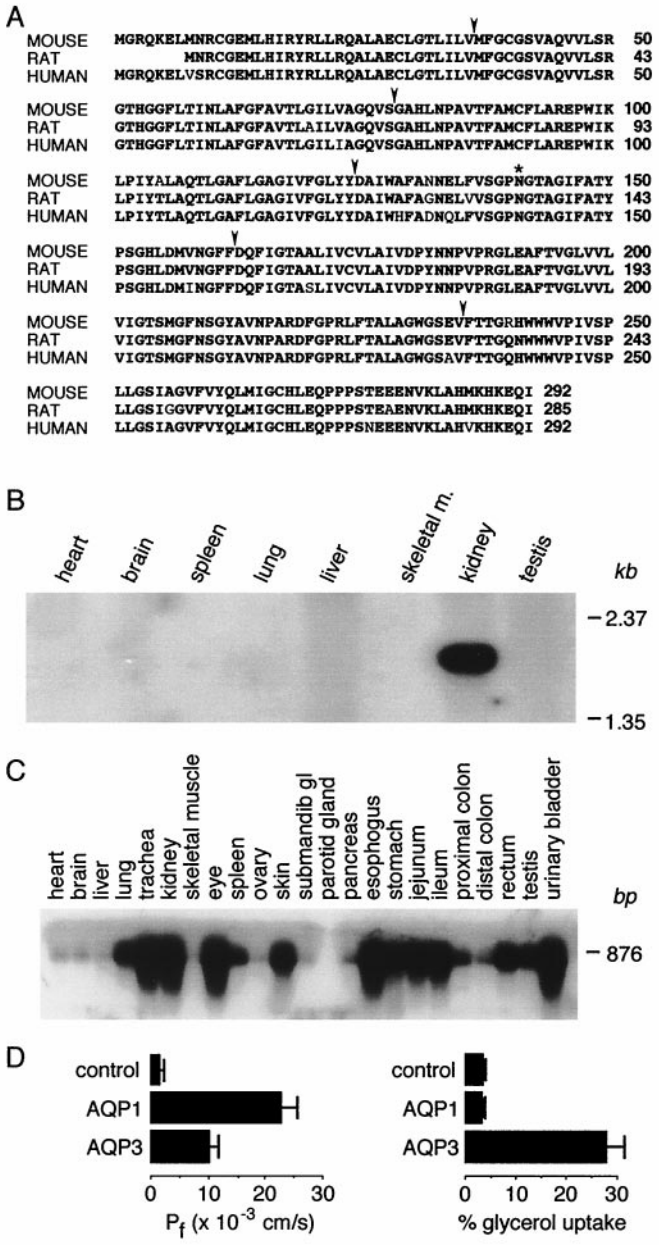

Fig. 1. Analysis of mouse AQP3 tissue distribution and function. (*A*) Comparison of deduced amino acid sequences of mouse, rat, and human AQP3. Conserved residues are shown in bold. Arrows, intron positions; *, glycosylation site. (*B*) Multitissue Northern blot probed with full-length AQP3 coding sequence. (*C*) Multitissue PCR/Southern blot showing AQP3 transcript distribution. (*D*) Osmotic water and glycerol permeabilities of control (water-injected) and mouse AQP1- and AQP3-expressing *Xenopus* oocytes.

located at residues 36, 79, 125, 164, and 237 in the deduced mouse AQP3 amino acid sequence, identical to the residues of the human AQP3 gene (13). Introns 1 and 4 are of class 0; introns 2 and 3 are of class 1; and intron 5 is of class 2. All boundaries (sequences deposited in GenBank database) correspond to the GT–AG^J rule. The upstream genomic sequence (to nucleotide −564) contains TATA box, SP1, and E-box elements but no cAMP response element. Genomic Southern blot analysis with *Eco*RI, *Hin*dIII, and *Xba*I-digested mouse genomic DNA indicated a single copy AQP3 gene per haploid mouse genome (not shown).

AQP3-knockout mice were generated by the targeting strategy shown in Fig. 2*A*. Heterozygous founder mice containing the disrupted AQP3 gene were bred to produce wild-type, heterozygous, and AQP3 null mice. Fig. 2*B* shows a genomic Southern blot confirming mouse genotype. Fig. 2*C* shows the absence of detectable AQP3 transcript in the null mice. As expected, AQP3 protein is expressed at the basolateral membrane of collecting-duct epithelial cells in wild-type mice but is absent in the null mice (Fig. 2*D*).

Genotype analysis of offspring from breeding of AQP3 heterozygous mice indicated a nearly 1:2:1 Mendelian distribution (105 wild-type, 226 heterozygous, and 118 null mice). Analysis of growth by animal weight (aged from 1 to 12 weeks) showed no differences among the genotypes. The AQP3 null mice have grossly normal appearance, activity, and behavior, but it was noted that cages housing AQP3 null mice had wet bedding because of high urine outputs. Light microscopic examination of hematoxylin/eosin-stained sections of kidney, trachea, eye, skin, urinary bladder, and lung indicated no gross morphological differences between wild-type and AQP3 null mice (not shown).

Renal function in AQP3 null mice was evaluated. In four pairs of wild-type and AQP3 null mice, serum concentrations of electrolytes (sodium: range 151–161 mM), urea (20–32 mg/dl), creatinine (0.1–0.2 mg/dl), calcium (9.3–10.9 mg/dl), and phosphorus (7.2–8.1 mg/dl) did not differ significantly; however, plasma osmolality was mildly elevated in AQP3 null mice (336.7 ± 2.8 vs. 329.6 ± 1.6; SEM; $n = 6$). Additional serum chemistries (liver functions, amylase, albumin, and cholesterol) were unremarkable except for hypotriglyceridemia (67 ± 13 mg/dl) in the AQP3 null mice compared with that in wild-type mice (130 ± 16 mg/dl).

The AQP3 null mice were markedly polyuric, consuming and excreting ≈10-fold more fluid than litter-matched heterozygous and wild-type mice (Fig. 3*A*). For comparison, mice lacking AQP1 consume approximately three times more fluid than wild-type litter mates, whereas AQP4 null mice are not polyuric (not shown; ref. 17). Average urine osmolality in AQP3 null mice [262 milliosmol (mosM)] was much lower than that in wild-type mice (1,270 mosM; Fig. 3*B*) or in mice lacking AQP1 (601 mosM; ref. 19) or AQP4 (1,399 mosM; ref. 17). It was postulated that deletion of AQP3 produces nephrogenic diabetes insipidus by decreasing the basolateral membrane water permeability of collecting duct such that transepithelial water transport is impaired. Urinary-concentrating ability was measured in response to DDAVP administration and to a 36-h water deprivation. Urine osmolalities in the AQP3 null mice increased significantly in each of these maneuvers, although to a much lesser extent than in wild-type mice. These results define a unique pattern of nephrogenic diabetes insipidus in AQP3 null mice that is quite different from that in AQP1 null mice where urine osmolality remains in the range of 600–700 mosM with water deprivation and DDAVP administration (19, 21).

The ability of AQP3 null mice to generate a partially concentrated urine in response to DDAVP or water deprivation may be due to functional AQP4 in distal segments of the collecting duct and/or to decreased luminal flow and slowed urine transit through the relatively water-impermeable collecting duct. To explore these possibilities, AQP3/AQP4 double-knockout mice were generated and analyzed. The double-knockout mice had grossly normal growth and phenotype except for marked polyuria (Fig. 3*A*). Urine osmolality was low when given free access to water and increased to a lesser extent than in AQP3 null mice in response to DDAVP administration and water deprivation (Fig. 3*B*; see *Discussion*).

To establish a cellular basis for the urinary-concentrating defect in AQP3-knockout mice, osmotic water permeability (P_f) was measured in basolateral membrane of cortical collecting duct by using spatial filtering microscopy. Collecting ducts were

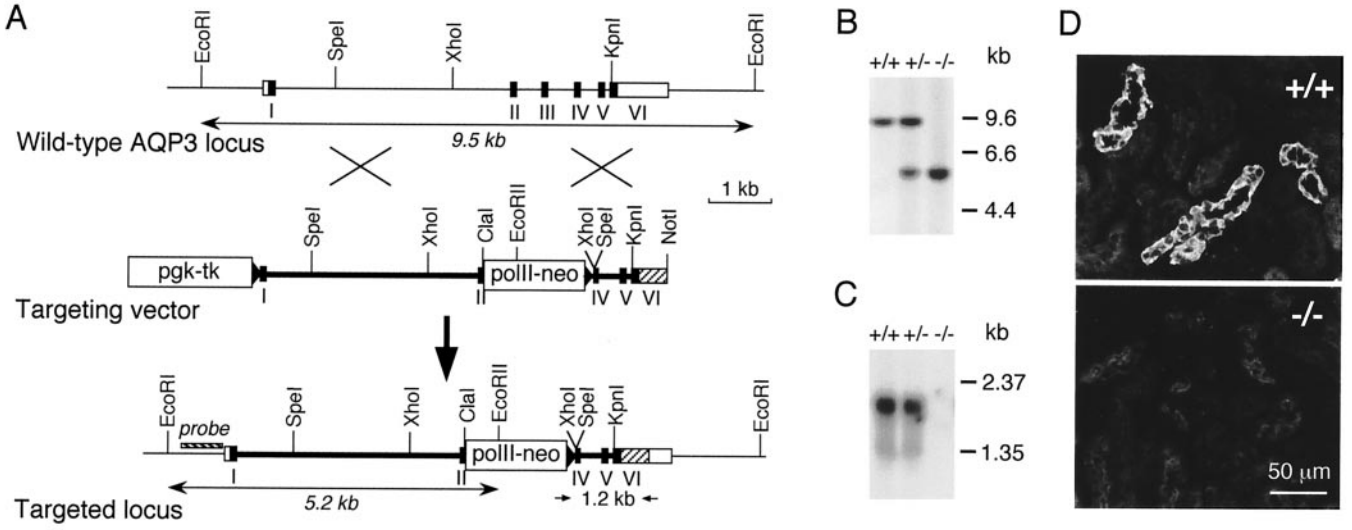

Fig. 2. Generation of AQP3 null mice. (*A Top*) Organization and restriction map of the mouse AQP3 gene based on PCR analysis, restriction digestion, and DNA sequencing. Rectangles indicate exon segments that constitute coding (filled) and untranslated (open) sequences. (*A Middle and Bottom*) Targeting strategy for AQP3 gene deletion. Homologous recombination results in replacement of the indicated segments of the AQP3 gene by a 1.8-kb polII-neo selectable marker. The probe used for Southern blot analysis is indicated (labeled ''probe''), and the 1.2-kb amplified region in PCR analysis is shown. (*B*) Southern blot of mouse liver genomic DNA digested with *Eco*RI and probed as indicated in *A*. (*C*) Northern blot of mouse kidney probed with the mouse AQP3 coding sequence. (*D*) Immunofluorescence localization of AQP3 protein in kidney cortex of wild-type (*Upper*) and AQP3 null (*Lower*) mouse.

immobilized on poly-D-lysine-coated cover glasses and superfused with isotonic and hypotonic solutions to induce reversible cell swelling. This approach provides information about basolateral membrane P_f, because the apical surface is not perfused. Fig. 4*A* shows rapid osmotically induced volume changes in cortical collecting ducts from wild-type mice, with a half-time ($t_{1/2}$) for osmotic equilibration of 1.09 ± 0.09 s, a few times slower than the system exchange time of ≈0.3 s. This rapid equilibration is comparable to that measured in microperfused collecting ducts from rabbit (26) and rat (27, 28) in which cell volume was deduced by tubule imaging, and perfusate exchange was accomplished in <0.1 s. Osmotic equilibration of collecting ducts from AQP3-knockout mice was significantly slower: 2.69 ± 0.1 s. Because of the finite solution exchange time in our system that might underestimate the rate in tubules from wild-type mice, it is concluded that AQP3 deletion produces at least a 3-fold decrease in water permeability of the basolateral membrane of cortical collecting duct. We did not compute absolute P_f values because of uncertainties in the basolateral membrane surface area exposed to the perfusate. Previous studies in rabbit cortical collecting duct indicated a convolved basolateral membrane that contributes to its high apparent water permeability (26).

Finally, the effect of AQP3 deletion on the expression of other renal aquaporins was investigated. Membrane homogenates from renal cortex and medulla were prepared from six well hydrated wild-type and AQP3 null mice. Immunoblot analysis of AQP2 protein showed significant down-regulation particularly in renal cortex (Fig. 4*B Upper*). Quantitative analysis showed only minor effects of AQP3 deletion on AQP1 and AQP4 protein

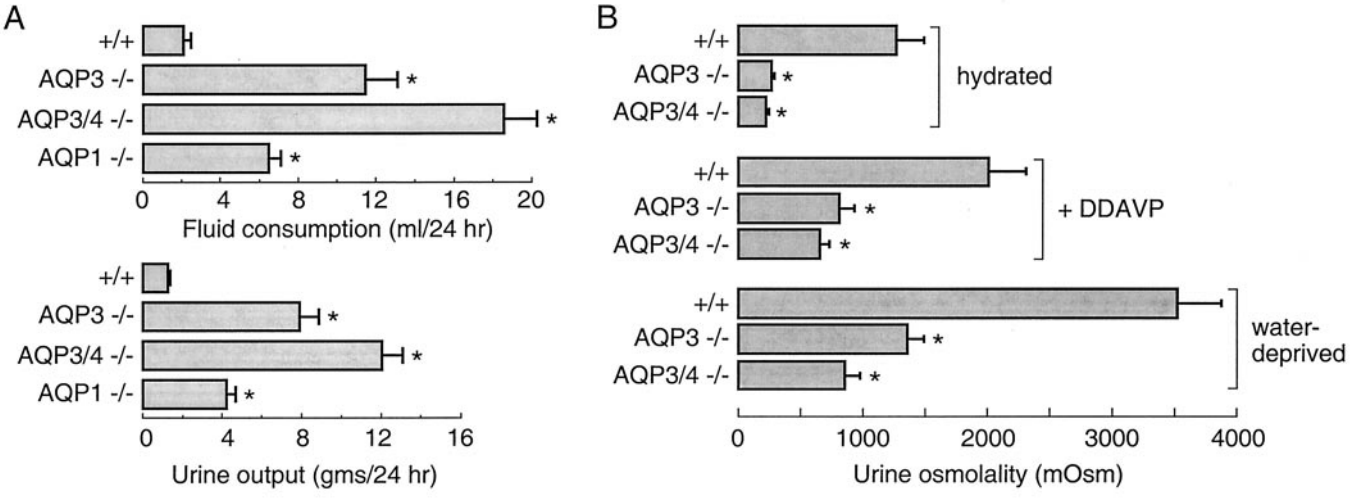

Fig. 3. Urinary-concentrating function in AQP3 single-knockout and AQP3/AQP4 double-knockout mice. (*A*) Fluid consumption (*Upper*) and urine output (*Lower*) over 24 h in mice of indicated genotype (SEM; 16 mice per genotype). (*B*) Urine osmolalities measured while mice were given free access to food and water before and after DDAVP administration and after a 36-h water deprivation (SEM; 12 mice per genotype). *, $P < 0.005$ compared with wild-type mouse.

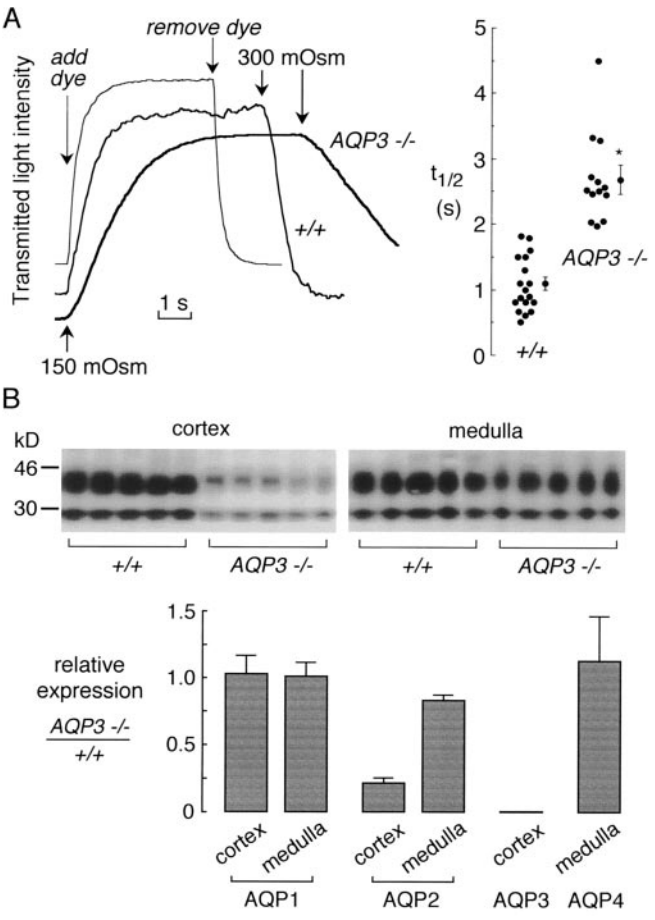

Fig. 4. Effect of AQP3 deletion on collecting-duct water permeability and expression of renal aquaporins. (*A*) Osmotic water permeability in basolateral membrane of cortical collecting ducts. (*A Left*) Representative time courses of collecting-duct cell volume (genotype indicated). Perfusion with hypoosmolar solution (150 mosM) produced cell swelling and increased transmitted optical signal. Perfusion exchange time (labeled ''add dye'' and ''remove dye'') was determined by absorbance of the dye Evans blue. (*A Right*) Averaged swelling rates for indicated mouse genotypes (SEM; *, $P < 0.001$). (*B*) Effect of AQP3 deletion on expression of renal aquaporin proteins. (*B Upper*) Immunoblot analysis of AQP2 in membranes from renal cortex and medulla from six wild-type and six AQP3-knockout mice. (*B Lower*) Quantitative densitometry of immunoblot data for indicated aquaporins.

expression and confirmed the significant down-regulation of AQP2. AQP2 down-regulation has been observed in various experimental models of nephrogenic diabetes insipidus including lithium administration, hypokalemia, hypercalcemia, and ureteral obstruction (reviewed in ref. 29).

Discussion

Despite its wide tissue distribution and ability to transport water as well as some small solutes, deletion of AQP3 in mice was not associated with impaired development, perinatal mortality, or growth retardation. In contrast, deletion of AQP1 and AQP5 in mice resulted in significant perinatal mortality, as demonstrated by the smaller than predicted number of offspring with the null genotype, as well as retarded growth compared with wild-type litter mates (19, 30). The only overt phenotype of the AQP3 null mice was marked polyuria with urine osmolalities substantially lower than those in wild-type mice or mice deficient in AQP1 or AQP4. The polyuria, urinary hypoosmolality, and partial response to V2 agonists in AQP3 null mice define a type of nephrogenic diabetes insipidus with a distinct physiological signature compared with that in AQP1-deficient mice or AQP2-deficient humans. Thus, AQP3 plays a key role in the urinary-concentrating mechanism, and its absence may account for some forms of nephrogenic diabetes insipidus in humans.

The impaired urinary-concentrating ability in AQP3 null mice indicates that the water permeability of the basolateral membrane of collecting duct can become a rate-limiting barrier when AQP3 is deleted. Indeed, water permeability in this membrane was at least 3-fold reduced in cortical collecting ducts of AQP3 null mice. The residual water permeability after AQP3 deletion is probably accounted for by lipid-mediated water transport across the convolved basolateral membrane surface (26, 31, 32). Although the *in vivo* findings are a consequence of AQP3 deletion in collecting duct, a number of compensatory changes and physiological issues must be considered. AQP3 null mice are remarkably polyuric and polydipsic when given free access to water. The normal functioning of the diluting segment, the high luminal flow, and the low collecting-duct water permeability in the diuretic kidney permit the excretion of a hypoosmolar urine. AQP2 down-regulation may contribute to the urinary hypoosmolality, and there may be compensatory changes in the expression/activity of various solute transporters. However, the AQP3 null mice were able to generate promptly a partially concentrated urine in response to DDAVP administration, well before changes in AQP2 expression could occur. Partial urinary-concentrating ability was also found after water deprivation. In contrast to AQP1 null mice, where the countercurrent exchange mechanism is defective, countercurrent exchange in AQP3 null mice is basically intact, although medullary interstitial osmolalities are probably lower than in wild-type mice because of diuresis washout. The generation of partially concentrated urine with a relatively water-impermeable collecting duct is a well documented phenomenon (33, 34) that is related to decreased glomerular filtration rate and low luminal flow in collecting duct. The low flow and consequent increased contact time facilitate osmotic extraction of water from the collecting-duct lumen.

Studies in double-knockout mice deficient in the two basolateral membrane water channels AQP3 and AQP4 provided further insight. It has been found that deletion of AQP4 produced a very mild defect in maximum urinary-concentrating ability (17) but a 4-fold decrease in transepithelial water permeability in the vasopressin-stimulated inner medullary collecting duct (18). The results reported herein support the notion that AQP4 and high inner medullary collecting-duct water permeability play only a minor role in the urinary-concentrating mechanism. The partial urinary-concentrating ability in the double-knockout mice in response to DDAVP or water deprivation is explained by the modest reduction in collecting-duct water permeability as discussed above.

In summary, the results reported herein implicate a key role of AQP3 in the urinary-concentrating mechanism, because its deletion is associated with nephrogenic diabetes insipidus. The AQP3 null mice should be useful in evaluating the role of AQP3 in upper airway and intestinal fluid transport, as well as in epidermal and conjunctival functions. The hypotriglyceridemia in AQP3 null mice may be related to the glycerol-transporting function of AQP3, as might the roles of AQP3 in skin, conjunctiva, and urinary bladder. Finally, the unambiguous renal phenotype of AQP3 and AQP3/AQP4 double-knockout mice should make them useful in studies of vector-mediated gene delivery to the kidney *in vivo*, as was done recently with AQP1 null mice (35).

We thank Ms. Liman Qain for mouse breeding and genotype analysis and Drs. Mark Knepper, Jurgen Schnermann, and Sei Sasaki for helpful advice and discussions. This work was supported by National Institutes of Health Grants DK35124, HL59198, HL60288, and DK43840 and Research Development Grant R613 from the National Cystic Fibrosis Foundation.

1. Ma, T., Frigeri, A., Hasegawa, H. & Verkman, A. S. (1994) *J. Biol. Chem.* **269,** 21845–21849.
2. Ishibashi, K., Sasaki, S., Fushimi, S., Uchida, S., Kuwahara, M., Saito, H., Furukawa, T., Nakajima, K., Yamaguchi, Y., Gojobori, T., *et al*. (1994) *Proc. Natl. Acad. Sci. USA* **91,** 6269–6273.
3. Echevarria, M., Windhager, E. E., Tate, S. S. & Frindt, G. (1994) *Proc. Natl. Acad. Sci. USA* **91,** 10997–11001.
4. Yang, B. & Verkman, A. S. (1997) *J. Biol. Chem.* **272,** 16140–16146.
5. Meinild, A. K., Klaerke, D. A. & Zeuthen, T. (1998) *J. Biol. Chem.* **273,** 32446–32451.
6. Kuwahara, M., Gu, Y., Ishibashi, K., Marumo, F. & Sasaki, S. (1997) *Biochemistry* **36,** 13973–13978.
7. Echevarria, M., Windhager, E. E. & Frindt, G. (1996) *J. Biol. Chem.* **271,** 25079–25082.
8. Frigeri, A., Gropper, M., Brown, D. & Verkman, A. S. (1995) *J. Cell Sci.* **108,** 2993–3002.
9. Frigeri, A., Gropper, M., Turck, C. W. & Verkman, A. S. (1995) *Proc. Natl. Acad. Sci. USA* **92,** 4328–4331.
10. Nielsen, S., King, L. S., Cristensen, B. M. & Agre, P. (1997) *Am. J. Physiol.* **273,** C1549–C1561.
11. King, L. S., Nielsen, S. & Agre, P. (1997) *Am. J. Physiol.* **273,** C1541–C1548.
12. Ramirez-Lorca, R., Vizuete, M. L., Venero, J. L., Revuelta, M., Cano, J., Ilundain, A. A. & Echevarria, M. (1999) *Pflügers Arch.* **438,** 94–100.
13. Inase, N., Fushimi, K., Ishibashi, K., Uchida, S., Ichioka, A., Sasaki, S. & Marumo, F. (1995) *J. Biol. Chem.* **270,** 17913–17916.
14. Ishibashi, K., Sasaki, S., Fushimi, K., Yamamoto, T., Kuwahara, M. & Marumo, F. (1997) *Am. J. Physiol.* **272,** F235–F241.
15. Ecelbarger, C. A., Terris, J., Frindt, G., Echevarria, M., Marples, D., Nielsen, S. & Knepper, M. A. (1995) *Am. J. Physiol.* **269,** F663–F672.
16. Terris, J., Ecelbarger, C. A., Marples, D., Knepper, M. A. & Nielsen, S. (1995) *Am. J. Physiol.* **269,** F775–F785.
17. Ma, T., Yang, B., Gillespie, A., Carlson, E. J., Epstein, C. J. & Verkman, A. S. (1997) *J. Clin. Invest.* **100,** 957–962.
18. Chou, C. L., Ma, T., Yang, B., Knepper, M. A. & Verkman, A. S. (1998) *Am. J. Physiol.* **274,** C549–C554.
19. Ma, T., Yang, B., Gillespie, A., Carlson, E. J., Epstein, C. J. & Verkman, A. S. (1998) *J. Biol. Chem.* **273,** 4296–4299.
20. Schnermann, J., Chou, C. L., Ma, T., Traynor, T., Knepper, M. A. & Verkman, A. S. (1998) *Proc. Natl. Acad. Sci. USA* **95,** 9660–9664.
21. Chou, C. L., Knepper, M. A., van Hoek, A. N., Brown, D., Yang, B., Ma, T. & Verkman, A. S. (1999) *J. Clin. Invest.* **103,** 491–496.
22. Pallone, T. L., Edwards, A., Ma, T., Silldorff, E. & Verkman, A. S. (2000) *J. Clin. Invest.* **105,** 2686–2692.
23. Zhang, R., Skach, W., Hasegawa, H., van Hoek, A. N. & Verkman, A. S. (1993) *J. Cell Biol.* **120,** 359–369.
24. Ma, T., Fukuda, N., Song, Y., Matthay, M. A. & Verkman, A. S. (2000) *J. Clin. Invest.* **105,** 93–100.
25. Farinas, J., Kneen, M., Moore, M. & Verkman, A. S. (1997) *J. Gen. Physiol.* **110,** 283–296.
26. Strange, K. & Spring, K. R. (1987) *J. Membr. Biol.* **96,** 27–43.
27. Flamion, B. & Spring, K. R. (1990) *Am. J. Physiol.* **259,** F986–F999.
28. Star, R. A. (1990) *J. Clin. Invest.* **86,** 1172–1178.
29. Marples, D., Frokiaer, J. & Nielsen, S. (1999) *Am. J. Physiol.* **276,** F331–F339.
30. Ma, T., Song, Y., Gillespie, A., Carlson, E. J., Epstein, C. J. & Verkman, A. S. (1999) *J. Biol. Chem.* **274,** 20071–20074.
31. Madsen, K. M. & Tisher, C. C. (1986) *Am. J. Physiol.* **250,** F1–F15.
32. Dorup, J. (1985) *J. Ultrastruc. Res.* **92,** 101–118.
33. Bennett, T. & Gardiner, S. M. (1987) *J. Physiol. (London)* **385,** 35–48.
34. Valtin, H. & Edwards, B. R. (1987) *Kidney Int.* **31,** 634–640.
35. Yang, B., Ma, T., Dong, J. Y. & Verkman, A. S. (2000) *Hum. Gene Ther.* **11,** 567–575.